NeuroImage: Clinical 25 (2020) 102141

Contents lists available at ScienceDirect

NeuroImage: Clinical

journal homepage: www.elsevier.com/locate/ynicl

# Microstructural damage of white-matter tracts connecting large-scale networks is related to impaired executive profile in alcohol use disorder

Chiara Crespi[a,b,*], Caterina Galandra[b], Nicola Canessa[a,b], Marina Manera[c], Paolo Poggi[d], Gianpaolo Basso[e]

[a] Scuola Universitaria Superiore IUSS Pavia, Piazza della Vittoria 15 27100, Pavia, Italy
[b] Cognitive Neuroscience Laboratory, IRCCS ICS Maugeri, 27100, Pavia, Italy
[c] Psychology Unit, IRCCS ICS Maugeri, 27100, Pavia, Italy
[d] Radiology Unit, IRCCS ICS Maugeri, 27100, Pavia, Italy
[e] University of Milano-Bicocca, 20126, Milan, Italy

ARTICLE INFO

*Keywords:*
Alcohol use disorder
White matter
Executive functions
Cognitive impairment
Large-scale brain networks
Rehabilitation

ABSTRACT

Alcohol Use Disorders (AUD) is associated with negative consequences on global functioning, likely reflecting chronic changes in brain morphology and connectivity. Previous attempts to characterize cognitive impairment in AUD addressed patients' performance in single domains, without considering their cognitive profile as a whole. While altered cognitive performance likely reflects abnormal white-matter microstructural properties, to date no study has directly addressed the relationship between a proxy of patients' cognitive profile and microstructural damage. To fill this gap we aimed to characterize the microstructural damage pattern, and its relationship with cognitive profile, in treatment-seeking AUD patients.

Twenty-two AUD patients and 18 healthy controls underwent a multimodal MRI protocol including diffusion tensor imaging (DTI), alongside a comprehensive neurocognitive assessment. We used a principal component analysis (PCA) to identify superordinate components maximally explaining variability in cognitive performance, and whole-brain voxelwise analyses to unveil the neural correlates of AUD patients' cognitive impairment in terms of different white-matter microstructural features, i.e. fractional anisotropy (FA), mean diffusivity (MD), axial diffusivity (AD) and radial diffusivity (RD).

PCA revealed a basic executive component, significantly impaired in AUD patients, associated with tasks tapping visuo-motor processing speed, attention and working-memory. Within a widespread pattern of white-matter damage in patients, we found diverse types of relationship linking WM microstructure and executive performance: (i) in the whole sample, we observed a linear relationship involving MD/RD metrics within both 'superficial' white-matter systems mediating connectivity within large-scale brain networks, and deeper systems modulating their reciprocal connections; (ii) in AUD patients vs. controls, a performance-by-group interaction highlighted a MD/AD pattern involving two frontal white-matter systems, including the genu of corpus callosum and cingulum bundle, mediating structural connectivity among central executive, salience and default mode networks.

Alterations of prefrontal white-matter pathways are suggestive of abnormal structural connectivity in AUD, whereby a defective interplay among large-scale networks underpins patients' executive dysfunction. These findings highlight different directions for future basic and translational research aiming to tailor novel rehabilitation strategies and assess their functional outcomes.

## 1. Introduction

Alcohol Use Disorder (AUD) is one of the most prevalent mental conditions worldwide (Grant et al., 2015; Rehm et al., 2015), with harmful consequences on individual's physical, cognitive and social functioning, reflecting in severe disability and difficulties in psychosocial adaptation (Bates et al., 2002; Grant et al., 2015; Zahr and Pfefferbaum, 2017).

The effects of chronic alcohol exposure involve both brain morphology and connectivity (De La Monte and Kril, 2014; C.

* Corresponding author.
*E-mail address:* chiara.crespi@iusspavia.it (C. Crespi).

https://doi.org/10.1016/j.nicl.2019.102141
Received 9 May 2019; Received in revised form 18 December 2019; Accepted 21 December 2019
Available online 23 December 2019

Galandra et al., 2018a, 2019), with widespread patterns of macro- and micro-structural changes mostly affecting frontal regions (Fortier et al., 2014) alongside diencephalic and hippocampal structures (De la Monte and Kril, 2014). Notably, such alcohol-related neurostructural effects have been mainly related to a reduction in white-matter (WM) volume (Fortier et al., 2014). Although the mechanisms driving alcohol-related WM loss are not completely understood, both neuropathological and neuroimaging studies showed that WM is particularly vulnerable to alcohol toxicity (De la Monte and Kril, 2014). The latter has been suggested to cause transitory and/or permanent damage (Yeh et al., 2009), ranging from transient changes in myelin sheet or axonal size to neural death by Wallerian degeneration (Oscar-Berman, 2000). In line with this view, *postmortem* studies associated prolonged alcohol consumption with an extensive damage of WM macro- and micro-structural properties, also including demyelination, microtubule disruption and axonal loss (Alhassoon et al., 2012). These changes primarily involve callosal, supratentorial and infratentorial regions, and the degree of WM loss reflects maximum daily alcohol consumption (Fortier et al., 2014).

Neuroimaging findings confirmed the prominent WM susceptibility to alcohol toxicity, as indicated by microstructural WM alterations in regions appearing unaltered on structural MRI (Sullivan and Pfefferbaum, 2003). In particular, considerable evidence highlights the corpus callosum as a consistent target of WM degeneration in AUD (e.g. Estruch et al., 1997; Fortier et al., 2014; Pfefferbaum et al., 2006; Zahr and Pfefferbaum, 2017). However, the microstructural damage observed in AUD involves a more widespread pattern, reflecting a decrease of fractional anisotropy (FA) in internal and external capsules, fornix, superior longitudinal fasciculus (Zahr and Pfefferbaum, 2017), as well as in fronto-limbic and fronto-cortical-striatal projections (Kuceyeski et al., 2013; Zou et al., 2018). In line with recent evidence on morphometric (Galandra et al., 2018a) and functional connectivity (Galandra et al., 2019) changes, these findings support the prominent vulnerability of frontal networks, in the context of a more diffuse WM microstructural damage, in AUD.

The observed relationship between cognitive impairment and neural damage in AUD is thus expected to involve also microstructural WM changes. This hypothesis is strengthened by distinct findings. First, there is consistent evidence of a significant relationship between microstructural properties and cognitive functions typically impaired in AUD (Bates et al., 2002; Glass et al., 2009; Le Berre et al., 2017). In particular, in AUD patients impaired decision-making performance – measured with the Iowa Gambling Task – has been linked to multiple indices reflecting the integrity of WM microstructure (i.e., FA, radial and axial diffusivities) in different sectors of corpus callosum, and in associative tracts of fronto-occipital and parietal lobes (Zorlu et al., 2013). Reduced memory performance in AUD patients has been related to FA in fronto-limbic bundles including the right cingulum and uncinate fasciculi, and bilateral inferior longitudinal fasciculus. Patients' deficits in executive performance (i.e., working-memory, attention, inhibition control) in AUD has been consistently correlated with multiple measures of microstructural integrity (FA, mean diffusivity, intravoxel coherence) in different sectors of the corpus callosum (Shulte et al., 2008; Pfefferbaum et al., 2010). Finally, executive dysfunction and psychomotor alterations in AUD, assessed with the Trial-Making Test, resulted significantly correlated with FA in anterior cingulum and motor areas (Konrad et al., 2012).

Second, such cognitive deficits reflect a possible breakdown of WM structures connecting regions in charge of executive processing. In particular, recent studies on AUD patients related a global proxy of basic executive functioning – involving psychomotor speed, attention and working memory performance – to the degree of atrophy in meso-cortico-limbic structures (Galandra et al., 2018a) and altered functional connectivity in fronto-striatal-limbic networks (Galandra et al., 2019). These findings suggested that AUD patients' executive impairment might reflect an abnormal switch between the *default-mode and central executive networks*, two anti-correlated brain systems associated with automatic vs. controlled effortful processing, when behaviorally relevant stimuli are detected by the *salience network* (Goulden et al., 2014; Menon and Uddin, 2010; Smith et al., 2009).

On this basis, we explored in the same sample studied in our previous works (Galandra et al., 2018a, 2019) a possible relationship between the cognitive profile in AUD (as indexed by a metric summarizing participants' performance in distinct executive tasks) and WM microstructural integrity in bundles connecting large-scale brain networks. This goal was first grounded in a detailed characterization of WM microstructural damage pattern, in terms of whole-brain voxelwise distribution of distinct DTI metrics identifying changes in the orientation coherence of water molecules diffusion (FA) and in the average amount of water diffusion (mean diffusivity or MD), as well as in radial (RD) and axial (AD) diffusivity indices which are supposed to reflect the degree of myelination and axonal damage/loss, respectively (Bennett et al., 2010). We then assessed whether WM damage can explain AUD patients' cognitive impairments, testing both linear correlations and performance-by-group interactions to better characterize the relationship between executive performance and WM microstructural alterations.

Previous related evidence suggests that the degree of executive impairment in AUD might reflect a widespread alteration of different DTI metrics, with a consistent involvement of callosal fibers exceeding the frontal cortex (Pandey et al., 2018; Zahr and Pfefferbaum, 2017). Based on our recent findings (Galandra et al., 2019, 2018a), we additionally expected that such relationship would involve damaged WM tracts connecting large-scale networks associated with executive control.

## 2. Material and methods

### 2.1. Participants

Twenty-two AUD patients and 18 healthy controls participated in the study, which included a semi-structured interview about alcohol and nicotine use habits, an extensive neuropsychological assessment, and a multimodal MRI scanning session. AUD patients were consecutively enrolled from the Functional Rehabilitation Unit of ICS Maugeri-Pavia (Italy), while healthy controls were recruited via local advertisement. The two groups were matched with respect to age, gender and education (see Table 1 for details).

Inclusion criteria for AUD patients were: age between 20 and 60 years, and a diagnosis of Alcohol Use Disorders according to DSM-5 criteria. Healthy controls were excluded in case of presence and/or history of alcohol abuse. Exclusion criteria for both groups were a) the presence and/or history of neurological/psychiatric disorders other than AUD, or any comorbid disorder except for nicotine dependence, b) family history of neurological/psychiatric disorders, c) current use of any psychotropic substance/medication, d) past brain injury or loss of consciousness, e) major medical disorders (e.g. kidney or liver diseases, sever diabetes and/or malnutrition), f) inability to undergo the neuropsychological assessment, and g) presence of contraindications to magnetic resonance imaging (MRI).

AUD patients joined the experimental protocol after being detoxified for at least 10 days by means of medically supported standard treatments. However, they had ceased benzodiazepine treatment at least 8 days before the MRI scanning. Healthy controls were abstinent at least 10 days before the MRI scanning.

All participants provided their written informed consent to the experimental procedure, which was approved by the Ethical Committee of ICS Maugeri (Pavia, Italy). The investigation was conducted in accordance with the latest version of the Declaration of Helsinki.

**Table 1**
Demographic, clinical and neurophysiological information. Section (a) reports demographic data concerning age, education, gender and smoking status of both AUD patients and healthy controls. Section (b) reports clinical information about alcohol use history and daily dose in AUD patients. Section (c) reports information about both global and single task scores (mean, standard deviation, range) related to neurocognitive performance obtained at the Brief Neuropsychological Exam-2 (ENB-2, Mondini et al., 2011) by AUD patients and healthy controls. We additionally reported details about statistics used for group comparisons and the relative results. (*) indicates results from non-parametric tests (Mann-Whitney U) used to investigate group comparisons in case of non-normally distributed data. In all the other cases, we assessed group differences with the Student's *t*-test for independent samples. AUD = AUD patients; HC = healthy controls; SD = standard deviation; TMT = Trail Making Test; *T* = Student's t-Test; *U* = Mann-Whitney U Test; FDR = False Discovery Rate adjustment applied on raw p-values.

| Group comparisons | | | | |
|---|---|---|---|---|
| (a) Demographic variables | | | | |
| | Mean ( ± SD, range) HC ($N$ = 18) | Mean ( ± SD, range) AUD ($n$ = 22) | T-score | p-value |
| Age (years) | 45 ( ± 8.9, 27–57) | 46 ( ± 8.0, 29–58) | −0.28 | 0.39 |
| Education (years) | 10 ( ± 2.8, 8–18) | 10 ( ± 2.6, 8–18) | 0.23 | 0.40 |
| Nicotine consumption (yes/no) | 6/12 | 18/4 | | 0.18 |
| (b) Alcohol use variables (patient group) | | | | |
| | Mean ( ± SD, range) | | | |
| Duration of alcohol use (years) | 10 ( ± 6.6, 1–26) | | | |
| Average daily alcohol dose (UA) | 14 ( ± 6.6, 5.6–32) | | | |
| Length of sobriety (days) | 14 ( ± 4.0, 6–21) | | | |
| (c) ENB Variables | | | | |
| ENB Subtest | Mean HC ( ± SD, range) | Mean AUD ( ± SD, range) | T/U* | FDR |
| Global Score | 84 ( ± 7, 69–96) | 78 ( ± 8, 59–90) | 2.6 | 0.021 |
| Digit Span | 5.78 ( ± 1, 4–8) | 5.72 ( ± 1, 3–8) | 184* | 0.42 |
| Immediate recall | 15( ± 5, 9–24) | 13 ( ± 4, 6–21) | 1.7 | 0.11 |
| Delayed recall | 20 ( ± 5, 11–28) | 19 ( ± 5, 7–28) | 1.01 | 0.32 |
| Interference memory 10″ | 7.6 ( ± 1.6, 4–8) | 6.2 ( ± 2, 1–9) | 105* | 0.02 |
| Interference memory 30″ | 7 ( ± 2, 2–9) | 6 ( ± 2, 2–9) | 169.5* | 0.36 |
| TMT-A | 19 ( ± 5, 11–28) | 29 ( ± 6, 14–40) | −5.41 | <0.001 |
| TMT-B | 68 ( ± 22, 41–115) | 85 ( ± 35, 45–208) | 132.5* | 0.11 |
| Token Test | 4.97 ( ± 0.1, 4.5–5) | 4.93 ( ± 0.2, 4.5–5) | 182* | 0.42 |
| Phonemic Fluency | 12.7 ( ± 3.1, 7–19) | 12.4 ( ± 3.3, 6.3–20) | 0.3 | 0.42 |
| Abstract verbal reasoning | 5.7 ( ± 1.0, 2–6) | 5.6 ( ± 0.9, 3–6) | 185.5* | 0.42 |
| Cognitive estimation | 4.722 ( ± 0.5, 4–5) | 4.727 ( ± 0.6, 3–5) | 190.5* | 0.42 |
| Overlapping figures | 37 ( ± 5.5, 24–46) | 31 ( ± 5.7, 20–41) | 3.27 | 0.006 |
| Copy drawing | 1.8 ( ± 0.4, 1–2) | 1.6 ( ± 0.6, 0–2) | 166.5* | 0.36 |
| Spontaneous Drawing | 1.9 ( ± 0.3, 1–2) | 1.7 ( ± 0.5, 0–2) | 174* | 0.4 |
| Clock Test | 9 ( ± 2.35, 0–10) | 8 ( ± 2.4, 0–10) | 102.5* | 0.018 |
| Praxic Abilities | 6 ( ± 0, 6–6) | 6 ( ± 0.2, 5–6) | 189* | 0.42 |

### 2.2. Clinical interview

All AUD patients were interviewed by an expert clinician about their drinking history, including the amount, type and lifetime duration of alcohol abuse. We used the average number of standard units of alcohol (UA) per day (1 UA = 330 ml beer, 125 ml wine, or 40 ml hard liquor = 12 g of ethanol) as a proxy of alcohol consumption (Table 1).

### 2.3. Neuropsychological assessment

We aimed to characterize participants' cognitive performance in different domains. To this purpose, both AUD patients and healthy controls underwent a 45 min neuropsychological assessment based on the Brief Neuropsychological Examination (ENB-2, Mondini et al., 2011), a well-validated battery for the Italian population including 15 tests assessing attention (trail making test, i.e. TMT-A and TMT-B), verbal short-term (digit span) and long-term (immediate and delayed prose memory) memory, working memory (10″ and 30″ interference memory), executive functions (TMT-B, cognitive estimation, abstract reasoning, phonemic fluency, clock drawing, overlapping pictures), perceptive and praxis skills (praxis abilities, spontaneous drawing, copy drawing task). The battery results in a global score, and in different subscores for each task.

### 2.4. Statistical analysis of neuropsychological data

The details on statistical analyses and neuropsychological data have been reported earlier (see Galandra et al., 2019, 2018a). Briefly, we used a multivariate approach based on a principal component analysis (PCA) to identify superordinate cognitive domains transcending single tasks and maximally explaining AUD patients' impairment. After assessing the suitability of the correlation matrix (Keiser-Meyer-Olkin Measure of Sampling Adequacy = 0.61; Bartlett's test of sphericity $<0.001$), we performed a PCA on the 15 ENB2 raw sub-scores. Due to the ambiguity of the scree plot, we used the Kaiser-Guttman criterion to determine the number of components to be retained (i.e., components with eigenvalue $>1$). An orthogonal rotation (Varimax) was used to facilitate the interpretation of components (Abdi and Williams, 2010). Finally, to investigate group differences in cognitive performance, we used an ANOVA (with Bonferroni correction for multiple comparisons) on the resulting factor scores of each component.

### 2.5. MRI protocol and DTI data acquisition

A 3 Tesla General Electrics Discovery MR750 scanner (GE Healthcare) with a 16-channel phased array head coil was used to run a multimodal MRI protocol, including a DTI sequence and a T2-weighted image (TR/TE = 7652/102 ms; FOV = 192 × 192 $mm^2$; 37 slices; bandwidth = 41,67 kHz; slice thickness = 4 mm, GAP = 0,2 mm) which was interpreted by an experienced neuroradiologist for diagnostic purposes. In particular, we acquired whole-brain DTI images using a single-shot echo planar sequence (TR/TE = 8986/80 ms; FOV = 256 × 256 $mm^2$; 56 sections; bandwidth = 250.0 kHz, 2 mm isotropic resolution), with diffusion gradients applied along 81 non-collinear directions (b-value = 1000 $s/mm^2$), and two non-diffusion weighted volumes.

### 2.6. DTI data preprocessing and analysis

We performed DTI data pre-processing and statistical analyses with the FMRIB Software Library tools (FSL; http://fsl.fmrib.ox.ac.uk/fsl/fslwiki/). Single-subject datasets were first corrected for eddy current distortions and motion artifacts, skull-stripped and finally, as a result of the fitting of the diffusion tensor model at each voxel, maps of diffusion scalar indices were generated. We then carried out DTI group analyses with Tract-Based Spatial Statistics (TBSS) (Smith et al., 2006), involving a voxelwise non-linear registration of fractional anisotropy (FA) maps of all subjects that, once aligned, were affine-transformed on a standard space ($1 \times 1 \times 1$ mm$^3$ MNI152). After co-registration, FA maps are averaged to create a mean FA image, and then used to generate a mean FA tract skeleton, representing all common tracts across subjects. We applied to the mean FA skeleton image a threshold of 0.20 to exclude from subsequent analysis those parts of the skeleton that could not ensure a good correspondence across subjects. Finally, to account for residual misalignments after the initial nonlinear registration, all subjects' FA data were projected onto the thresholded mean FA skeleton, creating a 4 D dataset of all subjects' FA skeletonized data. In addition, we ran the non-FA TBSS script on maps of mean (MD), axial (AD), and radial (RD) diffusivities. The resulting skeletonized data were then fed into whole-brain voxelwise statistical analyses.

Statistics were computed via *randomize*, a tool implementing a permutation-based non-parametric approach within the framework of the GLM. We used the Threshold-Free Cluster Enhancement (TFCE) option (Smith and Nichols, 2009) and set the significance threshold at $p<0.05$ corrected for multiple comparisons. We first tested the presence of white-matter microstructural alterations in AUD patients compared with healthy controls. To this purpose, we applied a two-group difference model (two-sample unpaired *t*-test) to each DTI metric, by setting a number of 5000 random permutations per contrast and including age as nuisance covariate. Then, we aimed to identify WM tracts showing a common pattern of microstructural alteration across all the indices under investigation. We thus generated a conjunction map by overlapping the distinct masks related to altered microstructure in AUD patients vs. healthy controls (FA: AUD < HC & MD: AUD > HC, & AD: AUD > HC, & RD: AUD > HC; all thresholded at $p<0.05$ corrected for multiple comparisons). We then extracted mean DTI indices from the significant clusters obtained both from voxelwise group analyses and from such common pattern, for off-line statistical analyses. Namely, we assessed a correlation between microstructural features and alcohol consumption variables (i.e., lifetime duration of alcohol abuse and daily alcohol consumption) in AUD patients.

Furthermore, we investigated the type of the relationship between cognitive performance and WM microstructural characteristics within the clusters displaying structural alterations in AUD patients. To this purpose, the results of the above voxelwise direct comparisons were used to create a binary mask reflecting the damage pattern in AUD patients vs. healthy controls for each DTI metric, and thus constrain subsequent analyses. Within the thereby obtained clusters, we first explored a relationship between white-matter microstructure and cognitive performance regardless of group. To this purpose, we tested a linear correlation, across both AUD and control groups, between each DTI metric and the factor scores of the PCA component showing a significant impairment in patients. We then estimated component-by-group interaction models to highlight possible qualitative group differences in the relationship between cognitive performance and WM microstructure in the clusters displaying structural alterations in AUD patients. In all these analyses the statistical threshold was set at $p<0.05$, TFCE corrected for multiple comparisons, with 5000 permutations per contrast.

The anatomical localization of significant clusters was performed using the JHU White-Matter Tractography Atlas and the JHU ICBM-DTI-81 White-Matter Labels (Hua et al., 2008). To provide a functional description of our findings in the framework of large-scale brain networks, we overlapped the significant result maps to the 12 white-matter functional networks identified by Peer and colleagues (Peer et al., 2017).

## 3. Results

### 3.1. Cognitive profile in AUD patients

Based on the Kaiser-Guttman criterion, considering components with eigenvalue >1, the neuropsychological dataset comprising the 15 ENB-2 variables was reduced to 6 components, explaining 76.42% of the overall variance. As previously reported (Galandra et al., 2019, 2018a), these components map onto different cognitive domains, i.e. visual-constructional abilities, verbal learning, basic-level and high-level executive processes, language and cognitive estimation. A strongly significant group difference in PCA factor scores was found in the third component (C3) ($F(1,38) = 12.15$, $p<0.005$), reflecting basic-level executive performance in the TMT-A (psychomotor speed and attention) and both 10″ and 30″ memory interference tests (working-memory). In particular, TMT-A provided the strongest contribution to this component ($r = -0.79$, $p<0.001$), followed by memory interference tasks (both $r = 0.72$, $p<0.001$).

### 3.2. White-matter microstructural damage in AUD patients

Whole-brain voxelwise analyses of DTI indices revealed a widespread damage of WM microstructural properties in AUD patients vs. healthy controls.

We found a significant FA alteration, with a restricted portion of the skeleton (3% of total skeleton voxels) showing a 12% reduction in AUD patients compared to healthy controls (Table 2). This pattern included the body of corpus callosum and projection fibers in the superior and posterior sectors of bilateral corona radiata, including the corticospinal tract. Small portions of the caudal parts of associative pathways (i.e., inferior fronto-occipital, inferior and superior longitudinal fasciculi) were also involved (Fig. 1, panel A; Figure S1).

In addition, we observed a widespread and co-localized pattern of alteration in MD, AD and RD (20–30% of total skeleton voxels), reflecting a significant increase of diffusivity indices (9–15%) in AUD patients compared to healthy controls (Table 2). Overall, this damage pattern encompassed commissural fibers (genu and body of corpus callosum, tapetum, forceps minor and forceps major), projection fibers (all sectors of corona radiata and internal capsule, encompassing the corticospinal tract and both the anterior and posterior thalamic radiations), and associative fibers (bilateral inferior and superior longitudinal fasciculi, inferior fronto-occipital fasciculus, uncinate fasciculus, fornix and left cingulum bundle) (Fig. 1, panel B; Figure S2).

The localization of significant results across all DTI metrics in terms of functionally characterized white-matter systems (Peer et al., 2017) highlighted the involvement of nine networks, including cingulum, sensorimotor system, forceps minor system, superior longitudinal fasciculus system, inferior longitudinal fasciculus system, inferior corticospinal tract, dorsal frontoparietal tracts, deep frontal WM, and

**Table 2**
Microstructural alteration in AUD patients vs. healthy controls.

| | | mean | SD | PV | t | p |
|---|---|---|---|---|---|---|
| FA | AUD | 0.52 | 0.04 | −12.37% | −5.946 | <0.0001 |
| | HC | 0.59 | 0.03 | | | |
| AD (x10-3, mm$^2$/s) | AUD | 1.30 | 0.08 | 9.11% | 3.402 | 0.002 |
| | HC | 1.19 | 0.12 | | | |
| MD (x10-3, mm$^2$/s) | AUD | 0.70 | 0.04 | 8.96% | 5.929 | <0.0001 |
| | HC | 0.73 | 0.03 | | | |
| RD (x10-3, mm$^2$/s) | AUD | 0.59 | 0.44 | 15.11% | 6.203 | <0.0001 |
| | HC | 0.51 | 0.03 | | | |

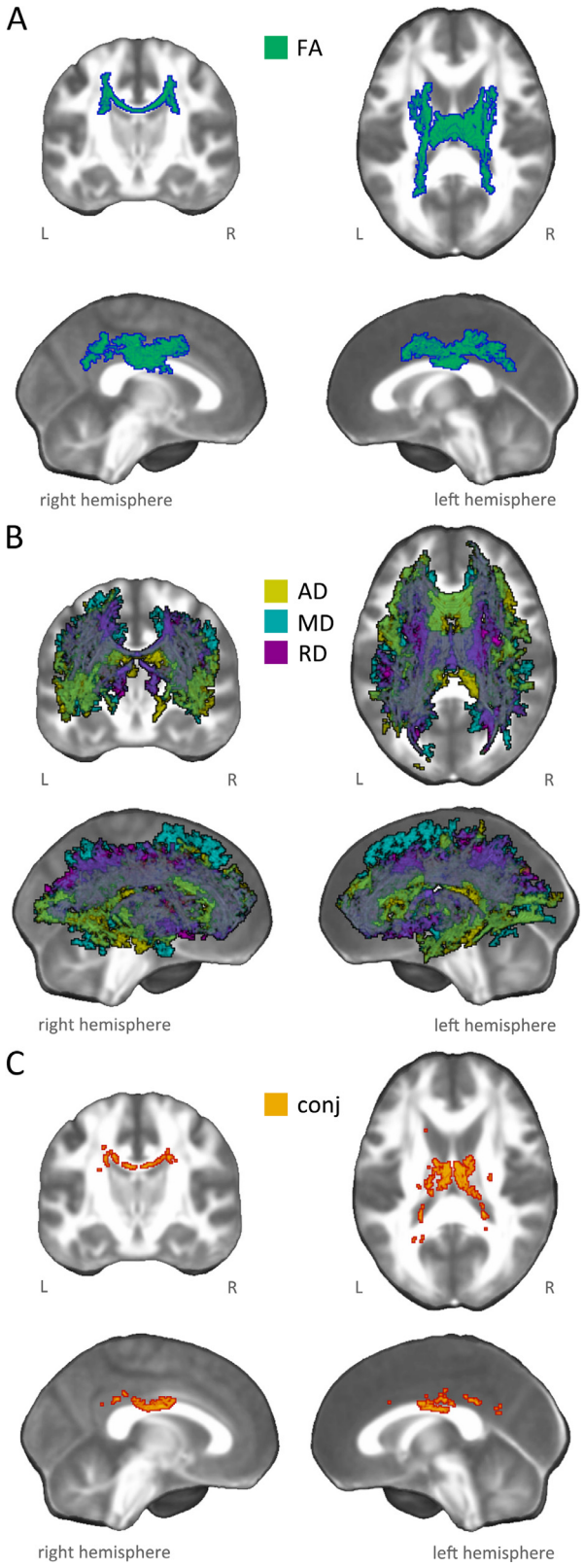


**Fig. 1.** White-matter microstructural damage in AUD patients. The figure illustrates significant group differences emerged from whole-brain voxelwise statistical analysis, highlighting microstructural changes in AUD patients compared to healthy controls. In particular, the different panels depict damage patterns reflecting: A) significant decrease in fractional anisotropy (FA: green-blue); B) significant increase in diffusivity indices (i.e. MD: light blue, AD: yellow, RD: purple); C) conjunction pattern (red-yellow) showing commonly altered regions in all DTI indices (i.e., FA: AUD < HC & MD: AUD > HC, & AD: AUD > HC, & RD: AUD > HC).

ventral frontoparietal tracts.

Finally, a conjunction analysis revealed an overlap of FA, MD, AD and RD damage in the body of corpus callosum (Fig. 1, panel C; Figure S3). The common pattern mainly involved two white-matter networks (Peer et al., 2017), namely the cingulum and the superior longitudinal fasciculus systems.

In AUD patients, the average DTI metrics extracted from the clusters showing group differences were significantly correlated (FDR corrected) with disease duration (FA: $r = -0.64$ $p = 0.004$; MD: $r = 0.57$ $p = 0.008$; AD: $r = 0.44$ $p = 0.04$; RD: $r = 0.61$ $p = 0.006$), but not with daily alcohol use (Figures S4-S7). Moreover, since disease duration was significantly correlated with patients' age ($r = 0.47, p = 0.027$) we performed a partial correlation analysis to control for the effect of age. The relationship between disease duration and microstructural alteration in AUD vs. healthy controls remained significant even after controlling for age variable for FA ($r = -0.51, p = 0.019$), MD ($r = 0.44$, $p = 0.046$) and RD ($r = 0.49$, $p = 0.025$) metrics. Also DTI metrics extracted from the conjunction map were significantly correlated only with disease duration (FA: $r = -0.56$ $p = 0.018$; MD: $r = 0.50$ $p = 0.023$; RD: $r = 0.55$ $p = 0.018$), and such a relationship remained significant after controlling for age for FA ($r = -0.50, p = 0.021$) and RD ($r = 0.45, p = 0.039$) metrics.

The table reports, for each microstructural metric explored, mean values extracted for group analysis (alteration patterns), as well as the relative standard deviation (SD), percent variation (PV) (decrease/increase in patients vs. controls), *t*-test statistic (t) and p-value (p). AUD = AUD patients; HC = healthy controls; FA = fractional anisotropy; AD = axial diffusivity; MD = mean diffusivity; RD = radial diffusivity.

### *3.3. Linear correlation between microstructural damage and basic executive performance*

Within the damage pattern observed in AUD patients, regardless of group the PCA factor score C3 reflecting basic executive performance was positively related to FA in the body of corpus callosum, and negative related to MD/RD in commissural fibers (genu, body and splenium of corpus callosum, forceps minor and forceps major), projection fibers (anterior, posterior and superior corona radiata, anterior and posterior thalamic radiations) and associative fibers (bilateral superior longitudinal, inferior longitudinal, inferior fronto-occipital and uncinate fasciculi, plus the cingulum bundle bilaterally) (Fig. 2; Figures S8-S10).

The overlap between functionally characterized white-matter networks (Peer et al., 2017) and significant results in FA, MD and RD revealed the involvement of eight networks, including the cingulum and the forceps minor systems, the superior longitudinal fasciculus system, the inferior longitudinal fasciculus system, the inferior corticospinal tract, deep frontal WM, plus dorsal and ventral fronto-parietal tracts.

### *3.4. Group-differences in the correlation between microstructural damage and basic executive performance (interaction analysis)*

Within the damage pattern observed in AUD patients we found evidence of a significant PCA component-by-group interaction effect on specific DTI metrics, with patients displaying a more negative relationship than controls between basic executive performance and both AD and MD metrics. These co-localized interaction patterns encompassed the genu and body of corpus callosum, the forceps minor, bilateral anterior corona radiata, as well as the anterior portions of associative fibers including the inferior fronto-occipital, inferior longitudinal and uncinate fasciculi, plus the left cingulum bundle (Fig. 3; Figures S11-S12).

The localization of these results in terms of functionally characterized white-matter networks (Peer et al., 2017) highlighted the involvement of two deep networks, including the forceps minor and the

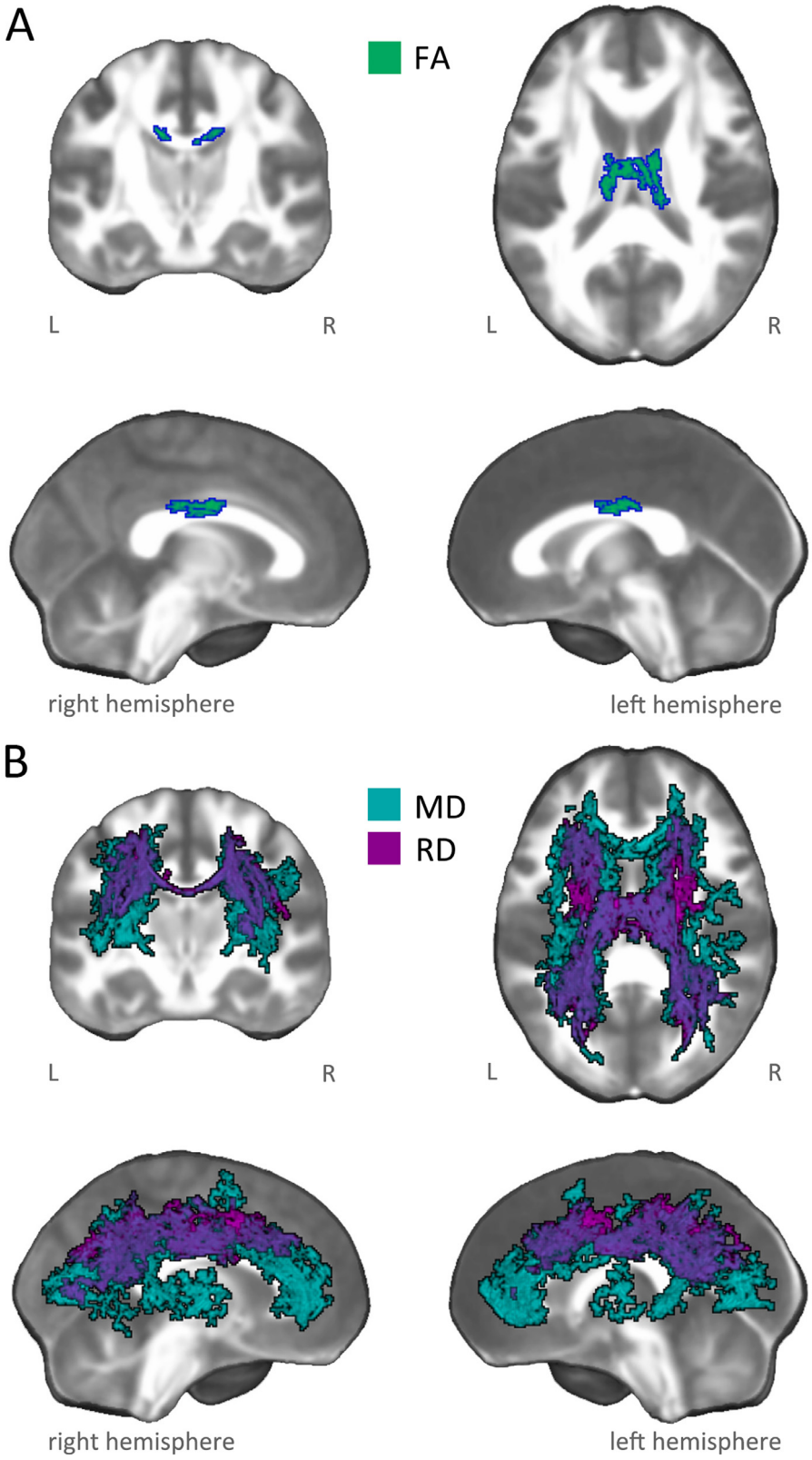


**Fig. 2.** Linear correlation between microstructural damage and basic executive performance. The figure shows white-matter patterns indicating a significant correlation between basic executive performance (i.e., C3) and microstructural indices in AUD patients and healthy controls, within damaged tracts observed in AUD patients. In particular, the panels depict: A) positive linear relationship between basic executive performance (i.e., C3) and fractional anisotropy (FA: green-blue); and B) negative linear relationship between basic executive performance (i.e., C3) and mean (MD: light blue) and axial (RD: purple) diffusivities.

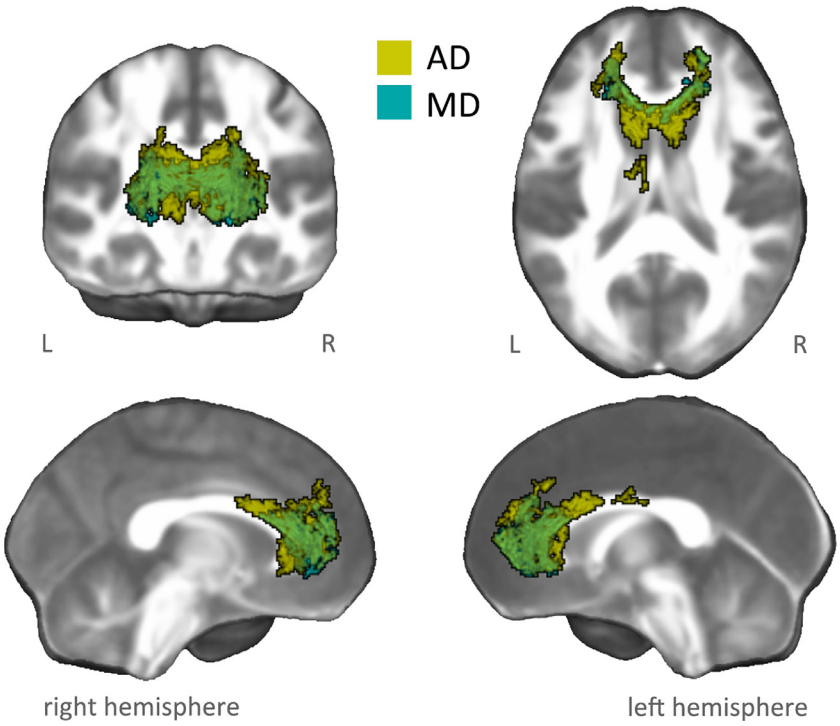


**Fig. 3.** Interaction analysis between microstructural damage and basic executive performance. The figure shows white-matter patterns indicating a performance-by-group interaction effect between basic executive performance (i.e., C3) and microstructural indices (MD: light blue, AD: yellow) in AUD patients vs. healthy controls, within damaged tracts observed in AUD patients. In particular, we observed a significant (negative) relationship between basic executive performance (i.e., C3) and MD/AD indices in AUD patients (MD: $r = -0.59$, $p = 0.004$; AD: $r = -0.45$, $p = 0.02$), but not in healthy controls (MD: $r = -0.04$, $p = 0.872$; AD: $r = 0.24$, $p = 0.338$).

deep frontal WM systems.

## 4. Discussion

We performed whole-brain voxelwise analyses of DTI metrics to characterize WM microstructural damage, and its relationship with basic executive dysfunction, in AUD patients compared with healthy controls. We explored WM metrics in the same sample studied in our previous works (Galandra et al., 2018a, 2019). Specifically, we investigated the distribution of fractional anisotropy (FA), previously used to explore WM microstructural damage in AUD (Fortier et al., 2014; Pfefferbaum et al., 2000; Pfefferbaum and Sullivan, 2005), alongside mean diffusivity (MD), axial diffusivity (AD) and radial diffusivity (RD), which are thought to reflect different facets of WM microstructural damage and/or degeneration. In particular, the altered microstructural integrity associated to FA changes has been ascribed to distinct processes affecting the orientation of water diffusion coherence within WM tissue (e.g., myelination or axon density) (Jones et al., 2013). Moreover, while MD represents a sensitive but relatively unspecific marker of WM degeneration, with its increase suggesting processes of density reduction in cell membranes (Beaulieu, 2002; Douaud et al., 2013), AD and RD changes are supposed to provide more specific information about the underlying neuropathological processes, related to axonal damage/loss and alteration of myelin sheets, respectively (Bennett et al., 2010).

We observed a widespread pattern of WM microstructural damage in all the diffusivity indices under investigation. These overlapping patterns massively involved genu and body of corpus callosum, as well as other commissural fibers (i.e., tapetum, forceps minor and forceps major), projection fibers encompassing the corticospinal pathway and thalamic radiations, as well as associative bundles, including the inferior and superior longitudinal fasciculi, inferior fronto-occipital fasciculus, uncinate fasciculus, fornix and cingulum bundle.

Unlike previous reports of widely decreased FA in AUD patients, also encompassing associative tracts (Fortier et al., 2014; Monnig et al., 2013), we observed localized FA reduction mainly in interhemispheric fibers within the body of corpus callosum, alongside projection fibers including the superior portions of the corticospinal pathway. While differences from previous studies might be ascribed to several factors, ranging from patients' characteristics to analytic pipelines, the significant increase of MD, AD and RD in AUD patients vs. controls supported previous evidence of a bilateral and diffuse pattern of microstructural alteration in AUD, which resulted positively related to disease duration. These data provide further confirm to the involvement of WM microstructure in AUD, and are in line with neuropathological findings that consistently found WM as a major target of alcohol toxicity (De la Monte et al., 2014).

Indeed, neuroimaging studies have shown that WM damage can exceed the overall pattern of gray matter atrophy (Pfefferbaum and Sullivan, 2002; Zahr and Pfefferbaum, 2017). Alongside our previous Voxel-Based Morphometry (VBM) findings, the present results on the same sample indeed support the higher sensitivity of DTI than morphometric measures in detecting neurostructural damage in AUD patients. While VBM results mostly involved core structures of the salience and executive networks (Galandra et al., 2018a), here we observed a widespread damage encompassing different WM systems. Microstructural alterations in AUD patients encompassed both *superficial WM systems* (functionally related to distinct gray matter networks such as frontoparietal control and attention networks, default mode network, sensorimotor, visual and cerebellar networks), and *deeper WM systems* (superior longitudinal fasciculus and dorsal fronto-parietal systems, inferior longitudinal fasciculus system, alongside deep frontal WM including forceps minor and anterior thalamic radiation). Although not directly connected to gray matter networks, the latter are thought to play a crucial role in cognitive functioning, by regulating their reciprocal connectivity (Peer et al., 2017).

In addition, the analysis of common damage patterns across FA and diffusivity indices consistently highlighted the microstructural alteration of corpus callosum as a core feature of AUD, possibly due to different degenerative processes affecting WM microstructure (Jones et al., 2013). The corpus callosum is the major WM system, connecting homologous regions of the two hemispheres. A degeneration, in terms of reduced thickness, of callosal interhemispheric fibers has been typically observed, particularly in the genu (connecting prefrontal regions) and body (connecting parietal and temporal lobes), in postmortem studies comparing alcoholic patients and controls

(Harper et al., 1988). This evidence was confirmed by in vivo neuroimaging studies, highlighting both macrostructural (e.g., volume reduction) and microstructural (e.g., FA decrease) changes in the corpus callosum (Estruch et al., 1997; Pfefferbaum et al., 2006; Schulte et al., 2004, 2005; Welch et al., 2013). In line with its role in interhemispheric communication and integration of sensory and cognitive information (van der Knaap and van der Ham, 2011), the degeneration of microstructural features of the corpus callosum has been shown to reflect, in AUD, in abnormal processing speed (Shulte et al., 2005, 2004), as well as in altered efficiency of cognitive functions such as working memory, attention, and visuo-spatial abilities (Jokinen et al., 2007; Pfefferbaum et al., 2006). In line with this evidence, here we show that a superordinate basic executive domain reflecting different facets of AUD patients' cognitive profile, such as psychomotor speed, attention and working memory, is associated with WM alterations.

First, regardless of group, executive performance was related to microstructural features within the WM sectors showing a significant damage in AUD patients. While in the case of FA this relationship mostly involved the body of corpus callosum, analyses on MD/RD displayed a more diffuse pattern, encompassing all sectors of the corpus callosum and several WM networks. In line with our previous reports on abnormal gray matter volume (Galandra et al., 2018a) and functional connectivity (Galandra et al., 2019), such relationship involved an extensive pattern including the cingulum, ventral fronto-parietal and inferior corticospinal systems. These WM systems, indeed, are known to connect key nodes of large-scale networks underlying the switch between automatic and controlled cognition and behavior, such as the default mode, ventral and dorsal attentional, fronto-parietal control and sensorimotor networks, alongside the anterior cerebellar network (Peer et al., 2017; Van Den Heuvel et al., 2009). Executive performance was also tracked by microstructural features of deeper WM systems connecting specific gray-matter networks (Peer et al., 2017), such as commissural (forceps minor and forceps major) and associative tracts connecting frontal regions with both parietal (superior longitudinal fasciculus) and temporo-occipital lobes (inferior longitudinal fasciculus, inferior fronto-occipital fasciculus). These findings fit with previous studies reporting a relationship between psychomotor, attentional and working-memory skills and both diffusivity and FA metrics in prefrontal, temporal and cingulum bundles (Crespi et al., 2018; Konrad et al., 2012; Makris et al., 2008; Pfefferbaum et al., 2010). This extensive correlational pattern involved specifically MD and RD metrics, possibly indicating that as the executive performance decrease water molecule diffusion and decreased myelination increase, respectively. While such alterations involved WM networks previously associated with altered goal-directed behavior in AUD patients, e.g. problem-solving (Stavro et al., 2013), cognitive flexibility (Chanraud et al., 2009) and decision-making (Galandra et al., 2018b; Zorlu et al., 2013), such a relationship seems to reflect group differences along a continuum from normal to impaired conditions.

Instead, a significant performance-by-group interaction revealed the presence of qualitative differences, between AUD patients and controls, in the relationship between cognitive performance and microstructural damage. Such interaction reflected a stronger relationship between impaired executive performance and increased MD/AD indices in AUD patients vs. controls. This pattern mainly involved the corpus callosum (genu and body), the forceps minor and the anterior portion of the cingulum bundle, as well as tracts belonging to deeper WM networks connecting fronto-temporal regions, such as the inferior fronto-occipital, inferior longitudinal and uncinate fasciculi (Peer et al., 2017). Among these bundles, the genu of corpus callosum and the cingulum are known to provide anatomical connectivity among the key nodes of large-scale functional networks (van den Heuvel et al., 2009). This finding is particularly relevant with respect to AUD patients' executive impairment, because functional alterations in these networks have been shown to reflect changes involving both their GM nodes and the WM tracts connecting them (Peer et al., 2017). In particular, the genu of corpus callosum connects homologous prefrontal regions, such as the dorsolateral prefrontal cortex (DLPFC), a key node of the central executive network (Voineskos et al., 2010), and the anterior cingulate cortex (ACC) (van der Knaap and van der Ham, 2011). Indeed, both the genu microstructure and DLPFC activity are linked to executive performance (Zahr et al., 2009), and previous neurophysiological evidence has shown the anatomical specificity of the relationship between genu microstructure and TMS-induced interhemispheric signal propagation from left to right DLPFC (Voineskos et al., 2010). The microstructural features of the genu are thus likely to shape the effectiveness of executive processes such as working-memory and cognitive control, which allow to actively maintain and manipulate information in the context of goal-directed behavior (Chen et al., 2013; Marstaller et al., 2015; Seeley et al., 2007). These processes are also supported by the same anterior portion of the cingulum bundle reported here, previously associated both with working-memory, attention and executive performance (Bubb et al., 2018; Kantarci et al., 2011; Metzler-Baddeley et al., 2012). Both the genu of the corpus callosum and the cingulum bundle project to the ACC, the unique common node between the default mode (Greicius et al., 2009) and salience (e.g., Chen et al., 2013; Marstaller et al., 2015; Seeley et al., 2007) networks, and functional connectivity within the DMN correlates with FA along the cingulum bundle (van den Heuvel et al., 2008).

By targeting a microstructural level of analysis, the present DTI findings complement our recent VBM (Galandra et al., 2018a) and functional connectivity (Galandra et al., 2019) data, and support the notion that executive deficits in AUD may reflect the selective damage of a salience-based neural mechanism enhancing the access to cognitive resources required for switching to controlled cognition and behavior. Here we addressed a deeper level of analysis, explaining such impairment in terms of microstructural damage in WM bundles mediating structural connectivity among the networks underlying the switch from automatic to controlled processing when salient stimuli/events are detected (Goulden et al., 2014; Sridharan et al., 2008). In particular, the relationship between basic executive performance and MD/AD indices highlights the role of alcohol-related axonal damage/loss in WM bundles mediating the interplay between default mode and frontal-parietal executive control networks. Besides explaining decreased processing speed in terms of a defective switch between these networks, such alterations are also likely to promote impulsivity and sub-optimal decision-making in AUD, when salient choice facets are not appropriately detected and processed (Galandra et al., 2018b; Grodin et al., 2017; Le Berre et al., 2017).

In the present study we have to report some crucial limitations. A first weakness is related to the small-to-moderate sample size, which underlines the need of confirmatory studies before strong conclusions can be drawn on the WM microstructural bases of impaired executive profile in AUD. This was mainly due to the strictness of inclusion criteria, the accurate case-control matching for demographic descriptors, as well as the control of other possible nuisance variables. A second limit refers to the lack of a precise quantification of the amount of smoke consumption, that would be have influenced our voxelwise results, especially for the fact that smoke has been proved to influence WM microstructure (e.g., Gons et al., 2011). In the present work, we did not model smoking habits as only qualitative information about the participants' smoking status are available, while a refined quantification of smoke exposure would require either the evaluation of nicotine blood-levels (Kochunov et al., 2013) or the administration of a structured interview (e.g., Fagerstorm Test for Nicotine Dependence, (Heatherton et al., 1991). Similarly, the method used here to calculate alcohol consumption in patients, rather than the administration of a validated questionnaire (e.g., Lifetime Drinking History), may have influenced the results about the lack of correlation between daily alcohol use and WM microstructure. Such a relationship has been reported in a few previous studies (e.g., Kril et al., 1997) but remains controversial, possibly due to the lack of consensus on the

quantification of daily alcohol use variable. However, the significant relationship we observed with lifetime alcohol consumption, which represents another facet of alcohol use habits in AUD, may be considered as a marker of the impact of alcohol exposure on WM microstructure. Another issue to keep into account is related to the limitations and pitfalls ascribable to the TBSS method, ranging from issues related to mis-assignments during the skeleton projection step to interpretation of significant results, as reported in Bach and colleagues (Bach et al., 2014). However, as recommended in that paper, our results were obtained by applying default parameter settings given by TBSS. The present conclusions are finally limited by the lack of specific measures of executive and attention control, preventing a refined assessment of the dysfunctional facets of AUD patients' performance in this cognitive domain. On the other hand, this limitation results from our explicit interest towards a comprehensive assessment of different cognitive domains, which, at the expense of specificity, allowed to highlight a superordinate executive domain transcending specific tasks. In this respect, the present study complements previous similar attempts to relate synthetic measures of cognitive proficiency with distinct metrics of brain functioning, such as brain metabolism (Goldstein et al., 2004), GM volume (Galandra et al., 2018a) and functional connectivity (Galandra et al., 2019). Importantly, in the trade-off between comprehensiveness and specificity, this approach unveiled a relationship between cognitive and microstructural alterations in AUD in terms of interacting networks rather than single tracts.

## 5. Conclusion

We provided novel evidence on the neural bases of defective executive performance in AUD. A detailed characterization of WM damage in AUD patients allowed to relate such impairment – primarily involving psychomotor speed, working-memory and attention – to different features of microstructural alteration in distinct bundles. The duration of alcohol abuse reflected in the degree of microstructural impairment at both the global (whole-brain) and local (corpus callosum) scales, which may be considered as an overall marker of disease history.

Additionally, executive performance was associated to different patterns of altered structural connectivity. The relationship between executive performance and microstructural WM features regardless of group, possibly reflecting individual differences in the degree of myelination, involved several WM tracts connecting large-scale networks such as ventral fronto-parietal and inferior corticospinal systems, alongside deeper WM systems connecting well-defined gray-matter networks (Peer et al., 2017). By showing group differences along a continuum from normal to impaired conditions, these data likely highlight the additional load of alcohol toxicity on several factors explaining individual differences in the relationship between microstructural WM integrity and executive performance. We also observed a specific relationship, in AUD patients, between executive performance and DTI metrics reflecting axonal damage or loss, mainly involving frontal WM networks. Among these, the involvement of the genu of corpus callosum and cingulum bundle supports an interpretation of AUD patients' executive impairment in terms of dysfunctional interplay among salience, default-mode and central executive networks, impairing the switch from automatic to controlled processing (Galandra et al., 2019, 2018a; Sullivan et al., 2013; Weiland et al., 2014).

The present results thus pave the way for future basic and translational research, including the identification of core components of executive dysfunction in AUD, to tailor novel intervention strategies, and the integration of multi-modal imaging data, to develop a comprehensive model of its anatomo-functional bases at multiple scales.

## CRediT authorship contribution statement

**Chiara Crespi:** Conceptualization, Methodology, Formal analysis, Writing - original draft, Writing - review & editing. **Caterina Galandra:** Conceptualization, Methodology, Investigation, Writing - review & editing. **Nicola Canessa:** Investigation, Writing - review & editing. **Marina Manera:** Investigation. **Paolo Poggi:** Writing - review & editing. **Gianpaolo Basso:** Conceptualization, Methodology, Investigation, Writing - review & editing.

## Declarations of Competing Interest

None

## Acknowledgments

We thank Dr. Giovanni Vittadini for his contribution in patient recruitment and clinical assessment.

## Supplementary materials

Supplementary material associated with this article can be found, in the online version, at doi:10.1016/j.nicl.2019.102141.

## References

Abdi, H., Williams, L.J., 2010. Principal Component Analysis – Abdi – 2010 – Wiley Interdisciplinary Reviews: Computational Statistics – Wiley Online Library. Wiley Interdiscip. Rev.

Alhassoon, O.M., Sorg, S.F., Taylor, M.J., Stephan, R.A., Schweinsburg, B.C., Stricker, N.H., Gongvatana, A., Grant, I., 2012. Callosal white matter microstructural recovery in abstinent alcoholics: a longitudinal diffusion tensor imaging study. Alcohol. Clin. Exp. Res. https://doi.org/10.1111/j.1530-0277.2012.01808.x.

Bach, M., Laun, F.B., Leemans, A., Tax, C.M.W., Biessels, G.J., Stieltjes, B., Maier-Hein, K.H., 2014. Methodological considerations on tract-based spatial statistics (TBSS). Neuroimage. https://doi.org/10.1016/j.neuroimage.2014.06.021.

Bates, M.E., Bowden, S.C., Barry, D., 2002. Neurocognitive impairment associated with alcohol use disorders: implications for treatment. Exp. Clin. Psychopharmacol.

Beaulieu, C., 2002. The basis of anisotropic water diffusion in the nervous system – A technical review. NMR Biomed. https://doi.org/10.1002/nbm.782.

Bennett, I.J., Madden, D.J., Vaidya, C.J., Howard, D.V., Howard, J.H., 2010. Age-related differences in multiple measures of white matter integrity: a diffusion tensor imaging study of healthy aging. Hum. Brain Mapp. https://doi.org/10.1002/hbm.20872.

Bubb, E.J., Metzler-Baddeley, C., Aggleton, J.P., 2018. The cingulum bundle: anatomy, function, and dysfunction. Neurosci. Biobehav. Rev. https://doi.org/10.1016/j.neubiorev.2018.05.008.

Chanraud, S., Reynaud, M., Wessa, M., Penttilä, J., Kostogianni, N., Cachia, A., Artiges, E., Delain, F., Perrin, M., Aubin, H.J., Cointepas, Y., Martelli, C., Martinot, J.L., 2009. Diffusion tensor tractography in mesencephalic bundles: relation to mental flexibility in detoxified alcohol-dependent subjects. Neuropsychopharmacology. https://doi.org/10.1038/npp.2008.101.

Chen, A.C., Oathes, D.J., Chang, C., Bradley, T., Zhou, Z.-W., Williams, L.M., Glover, G.H., Deisseroth, K., Etkin, A., 2013. Causal interactions between fronto-parietal central executive and default-mode networks in humans. Proc. Natl. Acad. Sci. https://doi.org/10.1073/pnas.1311772110.

Crespi, C., Laureiro-Martínez, D., Dodich, A., Cappa, S.F., Brusoni, S., Zollo, M., Falini, A., Canessa, N., 2018. Improving innovative decision-making: training-induced changes in fronto-parietal networks. Brain Cogn. 128. https://doi.org/10.1016/j.bandc.2018.11.004.

De La Monte, S.M., Kril, J.J., 2014. Human alcohol-related neuropathology. Acta Neuropathol. https://doi.org/10.1007/s00401-013-1233-3.

Douaud, G., Menke, R.A.L., Gass, A., Monsch, A.U., Rao, A., Whitcher, B., Zamboni, G., Matthews, P.M., Sollberger, M., Smith, S., 2013. Brain microstructure reveals early abnormalities more than two years prior to clinical progression from mild cognitive impairment to alzheimer's disease. J. Neurosci. https://doi.org/10.1523/JNEUROSCI.4437-12.2013.

Estruch, R., Nicolás, J.M., Salamero, M., Aragón, C., Sacanella, E., Fernández-Solà, J., Urbano-Márquez, A., 1997. Atrophy of the corpus callosum in chronic alcoholism. J. Neurol. Sci. https://doi.org/10.1016/S0022-510X(96)00298-5.

Fortier, C.B., Leritz, E.C., Salat, D.H., Lindemer, E., Maksimovskiy, A.L., Shepel, J., Williams, V., Venne, J.R., Milberg, W.P., Mcglinchey, R.E., 2014. Widespread effects of alcohol on white matter microstructure. Alcohol. Clin. Exp. Res. https://doi.org/10.1111/acer.12568.

Galandra, C., Basso, G., Cappa, S., Canessa, N., 2018b. The alcoholic brain: neural bases of impaired reward-based decision-making in alcohol use disorders. Neurol. Sci. https://doi.org/10.1007/s10072-017-3205-1.

Galandra, C., Basso, G., Manera, M., Crespi, C., Giorgi, I., Vittadini, G., Poggi, P., Canessa, N., 2018a. Salience network structural integrity predicts executive impairment in

alcohol use disorders. Sci. Rep 8. https://doi.org/10.1038/s41598-018-32828-x.
Galandra, C., Basso, G., Manera, M., Crespi, C., Giorgi, I., Vittadini, G., Poggi, P., Canessa, N., 2019. Abnormal fronto-striatal intrinsic connectivity reflects executive dysfunction in alcohol use disorders. Cortex 115. https://doi.org/10.1016/j.cortex.2019.01.004.
Glass, J.M., Buu, A., Adams, K.M., Nigg, J.T., Puttler, L.I., Jester, J.M., Zucker, R.A., 2009. Effects of alcoholism severity and smoking on executive neurocognitive function. Addiction. https://doi.org/10.1111/j.1360-0443.2008.02415.x.
Goldstein, R.Z., Leskovjan, A.C., Hoff, A.L., Hitzemann, R., Bashan, F., Khalsa, S.S., Wang, G.J., Fowler, J.S., Volkow, N.D., 2004. Severity of neuropsychological impairment in cocaine and alcohol addiction: association with metabolism in the prefrontal cortex. Neuropsychologia 42 (11), 1447–1458. https://doi.org/10.1016/j.neuropsychologia.2004.04.002.
Gons, R.A.R., Van Norden, A.G.W., De Laat, K.F., Van Oudheusden, L.J.B., Van Uden, I.W.M., Zwiers, M.P., Norris, D.G., De Leeuw, F.E., 2011. Cigarette smoking is associated with reduced microstructural integrity of cerebral white matter. Brain. https://doi.org/10.1093/brain/awr145.
Goulden, N., Khusnulina, A., Davis, N.J., Bracewell, R.M., Bokde, A.L., McNulty, J.P., Mullins, P.G., 2014. The salience network is responsible for switching between the default mode network and the central executive network: replication from DCM. Neuroimage. https://doi.org/10.1016/j.neuroimage.2014.05.052.
Grant, B.F., Goldstein, R.B., Saha, T.D., Patricia Chou, S., Jung, J., Zhang, H., Pickering, R.P., June Ruan, W., Smith, S.M., Huang, B., Hasin, D.S., 2015. Epidemiology of DSM-5 alcohol use disorder results from the national epidemiologic survey on alcohol and related conditions III. JAMA Psychiatry. https://doi.org/10.1001/jamapsychiatry.2015.0584.
Greicius, M.D., Supekar, K., Menon, V., Dougherty, R.F., 2009. Resting-state functional connectivity reflects structural connectivity in the default mode network. Cereb. Cortex. https://doi.org/10.1093/cercor/bhn059.
Grodin, E.N., Cortes, C.R., Spagnolo, P.A., Momenan, R., 2017. Structural deficits in salience network regions are associated with increased impulsivity and compulsivity in alcohol dependence. Drug Alcohol Depend. https://doi.org/10.1016/j.drugalcdep.2017.06.014.
Harper, C., Kril, J., Daly, J., 1988. Does a “moderate” alcohol intake damage the brain? J. Neurol. Neurosurg. Psychiatry. https://doi.org/10.1136/jnnp.51.7.909.
HEATHERTON, T.F., KOZLOWSKI, L.T., FRECKER, R.C., FAGERSTROM, K.-O, 1991. The fagerström test for nicotine dependence: a revision of the fagerstrom tolerance questionnaire. Br. J. Addict. https://doi.org/10.1111/j.1360-0443.1991.tb01879.x.
Hua, K., Zhang, J., Wakana, S., Jiang, H., Li, X., Reich, D.S., Calabresi, P.A., Pekar, J.J., van Zijl, P.C.M., Mori, S., 2008. Tract probability maps in stereotaxic spaces: analyses of white matter anatomy and tract-specific quantification. Neuroimage. https://doi.org/10.1016/j.neuroimage.2007.07.053.
Jokinen, H., Ryberg, C., Kalska, H., Ylikoski, R., Rostrup, E., Stegmann, M.B., Waldemar, G., Madureira, S., Ferro, J.M., Van Straaten, E.C.W., Scheltens, P., Barkhof, F., Fazekas, F., Schmidt, R., Carlucci, G., Pantoni, L., Inzitari, D., Erkinjuntti, T., 2007. Corpus callosum atrophy is associated with mental slowing and executive deficits in subjects with age-related white matter hyperintensities: the ladis study. J. Neurol. Neurosurg. Psychiatry. https://doi.org/10.1136/jnnp.2006.096792.
Jones, D.K., Knösche, T.R., Turner, R., 2013. White matter integrity, fiber count, and other fallacies: the do's and don'ts of diffusion MRI. Neuroimage. https://doi.org/10.1016/j.neuroimage.2012.06.081.
Kantarci, K., Senjem, M.L., Avula, R., Zhang, B., Samikoglu, A.R., Weigand, S.D., Przybelski, S.A., Edmonson, H.A., Vemuri, P., Knopman, D.S., Boeve, B.F., Ivnik, R.J., Smith, G.E., Petersen, R.C., Jack, C.R., 2011. Diffusion tensor imaging and cognitive function in older adults with no dementia. Neurology. https://doi.org/10.1212/WNL.0b013e31822313dc.
Kochunov, P., Du, X., Moran, L.V., Sampath, H., Andrea Wijtenburg, S., Yang, Y., Rowland, L.M., Stein, E.A., Elliot Hong, L., 2013. Acute nicotine administration effects on fractional anisotropy of cerebral white matter and associated attention performance. Front. Pharmacol. https://doi.org/10.3389/fphar.2013.00117.
Konrad, A., Vucurevic, G., Lorscheider, M., Bernow, N., Thümmel, M., Chai, C., Pfeifer, P., Stoeter, P., Scheurich, A., Fehr, C., 2012. Broad disruption of brain white matter microstructure and relationship with neuropsychological performance in male patients with severe alcohol dependence. Alcohol Alcohol. https://doi.org/10.1093/alcalc/agr157.
Kril, J.J., Halliday, G.M., Svoboda, M.D., Cartwright, H., 1997. The cerebral cortex is damaged in chronic alcoholics. Neuroscience. https://doi.org/10.1016/S0306-4522(97)00083-3.
Kuceyeski, A., Meyerhoff, D.J., Durazzo, T.C., Raj, A., 2013. Loss in connectivity among regions of the brain reward system in alcohol dependence. Hum. Brain Mapp. https://doi.org/10.1002/hbm.22132.
Le Berre, A.P., Fama, R., Sullivan, E.V., 2017. Executive functions, memory, and social cognitive deficits and recovery in chronic alcoholism: a critical review to inform future research. Alcohol. Clin. Exp. Res. https://doi.org/10.1111/acer.13431.
Makris, N., Oscar-Berman, M., Jaffin, S.K., Hodge, S.M., Kennedy, D.N., Caviness, V.S., Marinkovic, K., Breiter, H.C., Gasic, G.P., Harris, G.J., 2008. Decreased volume of the brain reward system in alcoholism. Biol. Psychiatry. https://doi.org/10.1016/j.biopsych.2008.01.018.
Marstaller, L., Williams, M., Rich, A., Savage, G., Burianová, H., 2015. Aging and large-scale functional networks: white matter integrity, gray matter volume, and functional connectivity in the resting state. Neuroscience. https://doi.org/10.1016/j.neuroscience.2015.01.049.
Menon, V., Uddin, L.Q., 2010. Saliency, switching, attention and control: a network model of insula function. Brain Struct. Funct. https://doi.org/10.1007/s00429-010-0262-0.
Metzler-Baddeley, C., Jones, D.K., Steventon, J., Westacott, L., Aggleton, J.P., O'Sullivan, M.J., 2012. Cingulum microstructure predicts cognitive control in older age and mild cognitive impairment. J. Neurosci. https://doi.org/10.1523/jneurosci.3299-12.2012.
Mondini, S., Mapelli, D., Vestri, A., Arcara, G., Bisiacchi, P., 2011. Esame neuropsicologico breve. Una Batteria Di Test Per Lo Screening Neuropsicologico. Raffaello Cortina.
Monnig, M.A., Tonigan, J.S., Yeo, R.A., Thoma, R.J., McCrady, B.S., 2013. White matter volume in alcohol use disorders: a meta-analysis. Addict. Biol. https://doi.org/10.1111/j.1369-1600.2012.00441.x.
Oscar-Berman, M., 2000. Neuropsychological Vulnerabilities in Chronic alcoholism., in: Review of NIAAA's Neuroscience and Behavioral Research Portfolio. National Institute on Alcohol Abuse and Alcoholism (NIAAA).
Pandey, A.K., Ardekani, B.A., Kamarajan, C., Zhang, J., Chorlian, D.B., Byrne, K.N.H., Pandey, G., Meyers, J.L., Kinreich, S., Stimus, A., Porjesz, B., 2018. Lower prefrontal and hippocampal volume and diffusion tensor imaging differences reflect structural and functional abnormalities in abstinent individuals with alcohol use disorder. Alcohol. Clin. Exp. Res. https://doi.org/10.1111/acer.13854.
Peer, M., Nitzan, M., Bick, A.S., Levin, N., Arzy, S., 2017. Evidence for functional networks within the human brain's white matter. J. Neurosci. https://doi.org/10.1523/JNEUROSCI.3872-16.2017.
Pfefferbaum, A., Adalsteinsson, E., Sullivan, E.V., 2006. Dysmorphology and microstructural degradation of the corpus callosum: interaction of age and alcoholism. Neurobiol. Aging. https://doi.org/10.1016/j.neurobiolaging.2005.05.007.
Pfefferbaum, A., Rosenbloom, M.J., Fama, R., Sassoon, S.A., Sullivan, E.V., 2010. Transcallosal white matter degradation detected with quantitative fiber tracking in alcoholic men and women: selective relations to dissociable functions. Alcohol. Clin. Exp. Res. https://doi.org/10.1111/j.1530-0277.2010.01197.x.
Pfefferbaum, A., Sullivan, E.V., 2002. Microstructural but not macrostructural disruption of white matter in women with chronic alcoholism. Neuroimage. https://doi.org/10.1006/nimg.2001.1018.
Pfefferbaum, A., Sullivan, E.V., 2005. Disruption of brain white matter microstructure by excessive intracellular and extracellular fluid in alcoholism: evidence from diffusion tensor imaging. Neuropsychopharmacology. https://doi.org/10.1038/sj.npp.1300623.
Pfefferbaum, A., Sullivan, E.V., Hedehus, M., Adalsteinsson, E., Lim, K.O., Moseley, M., 2000. In vivo detection and functional correlates of white matter microstructural disruption in chronic alcoholism. Alcohol. Clin. Exp. Res. https://doi.org/10.1111/j.1530-0277.2000.tb02086.x.
Rehm, J., Anderson, P., Barry, J., Dimitrov, P., Elekes, Z., Feijão, F., Frick, U., Gual, A., Gmel, Gerrit, Kraus, L., Marmet, S., Raninen, J., Rehm, M.X., Scafato, E., Shield, K.D., Trapencieris, M., Gmel, Gerhard, 2015. Prevalence of and potential influencing factors for alcohol dependence in europe. Eur. Addict. Res. https://doi.org/10.1159/000365284.
Schulte, T., Müller-Oehring, E.M., Javitz, H., Pfefferbaum, A., Sullivan, E.V., 2008. Callosal compromise differentially affects conflict processing and attentional allocation in alcoholism, HIV, and their comorbidity. Brain Imaging Behav. https://doi.org/10.1007/s11682-007-9014-z.
Schulte, T., Pfefferbaum, A., Sullivan, E.V., 2004. Parallel interhemispheric processing in aging and alcoholism: relation to corpus callosum size. Neuropsychologia. https://doi.org/10.1016/S0028-3932(03)00155-6.
Schulte, T., Sullivan, E.V., Müller-Oehring, E.M., Adalsteinsson, E., Pfefferbaum, A., 2005. Corpus callosal microstructural integrity influences interhemispheric processing: a diffusion tensor imaging study. Cereb. Cortex. https://doi.org/10.1093/cercor/bhi020.
Seeley, W.W., Menon, V., Schatzberg, A.F., Keller, J., Glover, G.H., Kenna, H., Reiss, A.L., Greicius, M.D., 2007. Dissociable intrinsic connectivity networks for salience processing and executive control. J. Neurosci. https://doi.org/10.1523/JNEUROSCI.5587-06.2007.
Smith, S.M., Fox, P.T., Miller, K.L., Glahn, D.C., Fox, P.M., Mackay, C.E., Filippini, N., Watkins, K.E., Toro, R., Laird, A.R., Beckmann, C.F., 2009. Correspondence of the brain's functional architecture during activation and rest. Proc. Natl. Acad. Sci. https://doi.org/10.1073/pnas.0905267106.
Smith, S.M., Jenkinson, M., Johansen-Berg, H., Rueckert, D., Nichols, T.E., Mackay, C.E., Watkins, K.E., Ciccarelli, O., Cader, M.Z., Matthews, P.M., Behrens, T.E.J., 2006. Tract-based spatial statistics: voxelwise analysis of multi-subject diffusion data. Neuroimage. https://doi.org/10.1016/j.neuroimage.2006.02.024.
Smith, S.M., Nichols, T.E., 2009. Threshold-free cluster enhancement: addressing problems of smoothing, threshold dependence and localisation in cluster inference. Neuroimage. https://doi.org/10.1016/j.neuroimage.2008.03.061.
Sridharan, D., Levitin, D.J., Menon, V., 2008. A critical role for the right fronto-insular cortex in switching between central-executive and default-mode networks. Proc. Natl. Acad. Sci. https://doi.org/10.1073/pnas.0800005105.
Stavro, K., Pelletier, J., Potvin, S., 2013. Widespread and sustained cognitive deficits in alcoholism: a meta-analysis. Addict. Biol. https://doi.org/10.1111/j.1369-1600.2011.00418.x.
Sullivan, E.V., Pfefferbaum, A., 2003. Diffusion tensor imaging in normal aging and neuropsychiatric disorders. Eur. J. Radiol.
Sullivan, E.V., Müller-Oehring, E., Pitel, A.L., Chanraud, S., Shankaranarayanan, A., Alsop, D.C., Rohlfing, T., Pfefferbaum, A., 2013. A selective insular perfusion deficit contributes to compromised salience network connectivity in recovering alcoholic men. Biol. Psychiatry. https://doi.org/10.1016/j.biopsych.2013.02.026.
van den Heuvel, M., Mandl, R., Luigjes, J., Hulshoff Pol, H., 2008. Microstructural organization of the cingulum tract and the level of default mode functional connectivity. J. Neurosci. https://doi.org/10.1523/jneurosci.2964-08.2008.
Van Den Heuvel, M.P., Mandl, R.C.W., Kahn, R.S., Hulshoff Pol, H.E., 2009. Functionally linked resting-state networks reflect the underlying structural connectivity architecture of the human brain. Hum. Brain Mapp. https://doi.org/10.1002/hbm.20737.

van der Knaap, L.J., van der Ham, I.J.M., 2011. How does the corpus callosum mediate interhemispheric transfer? A review. Behav. Brain Res. https://doi.org/10.1016/j.bbr.2011.04.018.

Voineskos, A.N., Farzan, F., Barr, M.S., Lobaugh, N.J., Mulsant, B.H., Chen, R., Fitzgerald, P.B., Daskalakis, Z.J., 2010. The role of the corpus callosum in transcranial magnetic stimulation induced interhemispheric signal propagation. Biol. Psychiatry. https://doi.org/10.1016/j.biopsych.2010.06.021.

Weiland, B.J., Sabbineni, A., Calhoun, V.D., Welsh, R.C., Bryan, A.D., Jung, R.E., Mayer, A.R., Hutchison, K.E., 2014. Reduced left executive control network functional connectivity is associated with alcohol use disorders. Alcohol. Clin. Exp. Res. https://doi.org/10.1111/acer.12505.

Welch, K.A., Carson, A., Lawrie, S.M., 2013. Brain structure in adolescents and young adults with alcohol problems: systematic review of imaging studies. Alcohol Alcohol. https://doi.org/10.1093/alcalc/agt037.

Yeh, P.H., Simpson, K., Durazzo, T.C., Gazdzinski, S., Meyerhoff, D.J., 2009. Tract-based spatial statistics (TBSS) of diffusion tensor imaging data in alcohol dependence: abnormalities of the motivational neurocircuitry. Psychiatry Res. – Neuroimaging. https://doi.org/10.1016/j.pscychresns.2008.07.012.

Zahr, N.M., Pfefferbaum, A., 2017. Alcohol's effects on the brain: neuroimaging results in humans and animal models. Alcohol Res.

Zahr, N.M., Rohlfing, T., Pfefferbaum, A., Sullivan, E.V., 2009. Problem solving, working memory, and motor correlates of association and commissural fiber bundles in normal aging: a quantitative fiber tracking study. Neuroimage. https://doi.org/10.1016/j.neuroimage.2008.09.046.

Zorlu, N., Gelal, F., Kuserli, A., Cenik, E., Durmaz, E., Saricicek, A., Gulseren, S., 2013. Abnormal white matter integrity and decision-making deficits in alcohol dependence. Psychiatry Res. – Neuroimaging. https://doi.org/10.1016/j.pscychresns.2013.06.014.

Zou, Y., Murray, D.E., Durazzo, T.C., Schmidt, T.P., Murray, T.A., Meyerhoff, D.J., 2018. White matter microstructural correlates of relapse in alcohol dependence. Psychiatry Res. – Neuroimaging. https://doi.org/10.1016/j.pscychresns.2018.09.004.